

Multiflavour excited mesons from the fifth dimension

Angel Paredes^a and Pere Talavera^b

^aCentre de Physique Théorique, Ecole Polytechnique,
91128 Palaiseau, France

^b Departament de Física i Enginyeria Nuclear,
Universitat Politècnica de Catalunya, Jordi Girona 1–3, E-08034 Barcelona, Spain

We study the Regge trajectories and the quark-antiquark energy in excited hadrons composed by different dynamical mass constituents via the gauge/string correspondence. First we exemplify the procedure in a supersymmetric system, D3-D7, in the extremal case. Afterwards we discuss the model dual to large- N_c QCD, D4-D6 system. In the latter case we find the field theory expected gross features of vector like theories: the spectrum resembles that of heavy quarkonia and the Chew-Frautschi plot of the singlet and first excited states is in qualitative agreement with those of lattice QCD. We stress the salient points of including different constituents masses.

December 2004

1. Motivation

One of the main features of vector-like theories is the self-interaction of the spin one gauge fields. With the inclusion of fundamental matter, colour charged, two competing contributions appears to the quark antiquark potential: one, attractive, is due to the interchange of the gauge bosons while the second, repulsive, comes from the self-interaction of these gauge bosons. The net effect is the formation of an electric flux between the two colour sources. The confined, electric flux tube connecting massless quarks can be modelled by a string, which represents one of the simplest hadron models [1,2]. When the string tension is constant it leads to a simple relation between the energy and the spin of the string, $E \sim \sqrt{J}$, *i.e.* Regge. From the quantum states assignment, Regge trajectories are based on flavour independence arguments and exchange degeneracy, *i.e.* J^{PC} and $(J+1)^{-P,-C}$ states belong to a common Regge trajectory. Even though it is well known that more realistic Regge behaviours include a positive curvature and a nonzero intercept [3].

It is our aim to recast the features of these models in the gravity/field theory duality framework. For that purpose we shall deal with the meson Regge trajectory in the light of holographic duals of confining supergravity backgrounds. In the first holographic setup [4,5] the addition of matter was achieved by higgsing the initial gauge group: A stack of N D3-branes was considered at the origin giving rise to a gauge group $SU(N)$. Then one of the branes was pulled out up to the boundary breaking the initial gauge group to $SU(N-1) \times U(1)$. The string length stretching from the origin up to the boundary is proportional to the mass of the quark attached at one of the string ends. Then the final picture was an infinite heavy quark at the boundary. Considering two of such strings a more stable configuration, merging the lower end points, is possible giving a bound state of two infinite masses.

The addition of finite flavoured matter is achieved by means of an open string sector [6]. The end points of these are supported by N_f nonbackreacting filling space-time D-branes, $N_f \ll N_c \rightarrow \infty$. In most of the cases, D-branes carry RR-gauge fields and hence a nonzero charge. A possible mechanism to stabilise them at finite distance is by wrapping trivial cycles [7,8]. Then, without creating instabilities, negative massive modes prevent the slipping of the D-brane out of the wrapped trivial cycle. The final result are a set of mesons (in the large- N_c limit) consisting of bound state poles. Neglecting meson widths correspond to disregard mixing between $q\bar{q}$ and other sectors of the theory as glueballs or $qq\bar{q}\bar{q}$.

The meson spectrum can be divided in two different sectors: *i)* A sector with small ($J = 0, 1, 2$) angular momentum, that can be tackled considering small fluctuations of the probe-brane. *ii)* Stringy states at large- J corresponding to excited meson states. In

the latter case they are represented by rotating Wilson-loops. Notice that this inherently implies a semi-classical limit. It is then natural to assume that isolated hadrons exist at sufficient energy to be treated semi-classically [9].

We shall consider the spectrum of the stringy states in a generic case: an hadron formed by two different constituents masses. This will allow us to study some features of the hadron excited spectra as a function of the masses in a more realistic set up. There is, for instance, little knowledge of heavy-light charmed mesons. While at low-energy there is no significant change with respect to the degenerate case, at high-energy the entire profile changes. In the cases where the metric has been obtained via compactification we argue that in the vicinity of the high-energy region there is the opening of the compactified dimensions, and hence the dual field theory is changed.

In order to introduce notation and the main work line we deal with an extremal supersymmetric model, D3-D7. We discuss the spectrum, the energy-momenta relation and the quark-antiquark energy. We pay especial attention to the role of mass subtraction. We turn then to evaluate the above features in a nonsupersymmetric model, D4-D6, comparing their qualitative behaviour with the experimental ones. In addition we comment on the quark-antiquark potential screening and on the 't Hooft line.

Even if we treated $\mathcal{N} = 2$ and $\mathcal{N} = 0$ theories it would also be interesting to perform a similar analysis for $\mathcal{N} = 1$ theories although, being confining, it is natural to expect a similar behaviour to that of the non-supersymmetric case. The embedding of the corresponding flavour branes was studied [10] in the case of a non-conformally flat setup and in [11,12,13] for the theories on the conifold.

2. The $D3 - D7$ brane model

We start with a supersymmetric system that allows a fairly good analytic control over the full calculation. To obtain a system with matter in the bi-fundamental representation we make use of the observation that a holographic dual to 4-dimensional super-Yang-Mills (SYM) theory can be obtained in the near-horizon limit of the D3-D7 system [6].

The set up consists in a stack of N_c D3-branes at the origin expanding in four-directions $(0, 1, 2, 3)$ and warping along the transverse ones. This give rise to an $\mathcal{N} = 4$ SYM field theory. Another set of N_f D7-branes are located along $(0, 1, 2, 3, 4, 5, 6, 7)$ and warping in the rest of dimensions. The insertion of this last stack of branes breaks the initial $\mathcal{N} = 4$ symmetry to $\mathcal{N} = 2$ SYM at low-energy. We shall consider the case $N_f \ll N_c$, then the D7-brane backreaction can be ignored.

The D3-brane system can be obtained from type-IIB string theory on the $AdS_5 \times S^5$

background

$$ds^2 = f(U)^{-1/2} (-dx_0^2 + d\vec{x}^2) + f(U)^{1/2} d\vec{y}^2, \quad f(U) = \frac{\mathcal{R}^4}{U^4}, \quad (2.1)$$

with $\vec{x} = (x_1, x_2, x_3)$, $\vec{y} = (x_4, \dots, x_9)$, $\rho^2 = \vec{y}^2$ and $\mathcal{R}^2 = \sqrt{4\pi g_s N_c} \alpha'$. The induced metric on the D7-brane embedding is that of $AdS_5 \times S^3$, i.e. the D7 fills all the AdS space but is only a contractible cycle on S^5 . This breaks the initial $SO(6)$ symmetry on the S^5 to $SO(4) \times SO(2)$. The former corresponds to the isometry group of the S^3 while the latter to the rotations on the (x_8, x_9) plane.

The fundamental massive gauge theory is found by separating, a distance ℓ , the D7-branes in the $x_8 - x_9$ plane, $x_8^2 + x_9^2 = \ell^2$

$$ds^2 = \frac{U^2 + \ell^2}{\mathcal{R}^2} (-dx_0^2 + d\vec{x}^2) + \frac{\mathcal{R}^2}{U^2 + \ell^2} d\Omega_4^2, \quad d\Omega_4^2 = (dU^2 + U^2 d\Omega_3^2). \quad (2.2)$$

In flat Minkowsky space the quark mass is proportional to ℓ . At the ultraviolet region, $U \gg \ell$, (2.2) asymptotes to $AdS_5 \times S^3$ providing a conformal invariant gauge theory. In reducing the energy, decreasing U , conformal invariance is lost.

2.1. Spinning mesons

We start by determining the possible spectrum for open rotating strings with ends attached to the D7-branes \natural . The string worldsheet action is parametrised by (τ, σ) as

$$S = \int d\tau d\sigma \mathcal{L}(X, \partial_\sigma X, \partial_\tau X). \quad (2.3)$$

The string configuration we choose is the same as the one described in [15] but with the insertion of a second brane probe. It will lie at a fixed point in S^5 , rotating with constant angular velocity ω within a 2-plane in E^3 and extending in the direction $z = \mathcal{R}^2/U$. The relevant part of the metric is then

$$ds^2 = \frac{\mathcal{R}^2}{z^2} (-dt^2 + dr^2 + r^2 d\theta^2 + dz^2). \quad (2.4)$$

Defining z_{m_q} as the position of the flavour brane in terms of the new coordinate z , the mass of the quark is

$$m_q = \frac{\mathcal{R}^2}{2\pi z_{m_q}}. \quad (2.5)$$

\natural The chiral symmetry breaking of the model was studied in [14].

The rotating string describes a cigar-like surface with the configuration

$$t = \kappa \tau, \quad r(\sigma), \quad \theta = \omega \tau, \quad z(\sigma). \quad (2.6)$$

Under the latter assumption, (2.6), the Lagrangian density takes the form

$$\mathcal{L} = -\frac{\mathcal{R}^2}{2\pi\alpha'} \frac{1}{z^2} \sqrt{(\kappa^2 - \omega^2 r^2)(z'^2 + r'^2)}, \quad (2.7)$$

where we have already substituted ω for $\dot{\theta}$ and denoted ∂_σ by primes. The equations of motion for $z(\sigma)$ and $r(\sigma)$ are equal and they reduce to

$$\frac{1}{z'^2 + r'^2} (z' r'' - z'' r') + \omega^2 \frac{r}{\kappa^2 - \omega^2 r^2} z' - 2 \frac{r'}{z} = 0. \quad (2.8)$$

In addition to (2.8) one has to supplement the system with the proper set of boundary conditions (b.c.). In order to find the b.c. to be applied we use the minimum action principle: the string must be stationary under small deformations of the world-line

$$\begin{aligned} \delta S = & -2 \int d\tau d\sigma \delta z \frac{1}{z^3} \sqrt{(\kappa^2 - \omega^2 r^2)(r'^2 + z'^2)} - \omega^2 \int d\tau d\sigma \delta r \frac{r}{z^2} \sqrt{\frac{r'^2 + z'^2}{\kappa^2 - \omega^2 r^2}} \\ & + \int d\tau \delta r \frac{r'}{z^2} \sqrt{\frac{\kappa^2 - \omega^2 r^2}{r'^2 + z'^2}} \Big|_{\sigma=-\pi/2}^{\sigma=\pi/2} + \int d\tau \delta z \frac{z'}{z^2} \sqrt{\frac{\kappa^2 - \omega^2 r^2}{r'^2 + z'^2}} \Big|_{\sigma=-\pi/2}^{\sigma=\pi/2} = 0. \end{aligned} \quad (2.9)$$

Each end of the string lies on one of the D7 branes, *i.e.* z -coordinates obey Dirichlet b.c. While for (2.6) r obeys a Neumann b.c. . From (2.9) and in the case of subluminal velocities this implies that the string ends hit the D7-brane orthogonally.

The e.o.m. are easily worked out by fixing the gauge

i) $r(\sigma) = \sigma$

$$\frac{z''}{1 + z'^2} - \frac{\omega^2 \sigma}{1 - \omega^2 \sigma^2} z' + \frac{2}{z} = 0. \quad (2.10)$$

ii) $z(\sigma) = \sigma$

$$\frac{r''}{1 + r'^2} - 2 \frac{r'}{\sigma} + \frac{\omega^2}{1 - \omega^2 r^2} r = 0. \quad (2.11)$$

Notice that (2.10), (2.11) are identical to the ones given in [15]. Our only concern here has to do with the b.c. imposed on these

$$z_{m_q}, z_{M_q} = \text{fixed}, \quad \partial_\sigma z|_{\sigma=\pm\frac{\pi}{2}} \rightarrow \infty. \quad (2.12)$$

In the limiting case, $z_{m_q} = z_{M_q}$ we recover the results presented in [15].

The system (2.7) does not depend explicitly neither on the time coordinate nor on θ . This implies the existence of two conserved quantities. Moreover using reparametrisation invariance, $\kappa = 1$, the energy and the spin are given by

$$E = \frac{\mathcal{R}^2}{2\pi\alpha'} \int d\sigma \frac{1}{z^2} \sqrt{\frac{z'^2 + r'^2}{1 - \omega^2 r'^2}}, \quad (2.13)$$

$$J = \frac{\mathcal{R}^2 \omega}{2\pi\alpha'} \int d\sigma \left(\frac{r}{z}\right)^2 \sqrt{\frac{z'^2 + r'^2}{1 - \omega^2 r'^2}}. \quad (2.14)$$

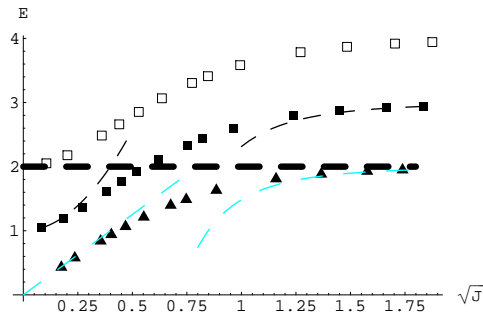


Fig. 1: Chew-Frautschi plot for $m_q = 1$ and $M_q = 1, 2, 3$. The dashed lines represent the limits (2.18) and (2.29) for the equal and degenerate case. We also have plotted (horizontal thick line) the energy of a free system of quarks of energy $2m_q$.

We shall study the behaviour of (2.10), (2.11), (2.13) and (2.14). The most straight forward way is a numerical analysis. In fig. 1 we show the energy versus the squared root of the angular momentum \mathfrak{J} . As one can see the degenerate system behaves at low-angular momenta in a completely different manner as the different masses case. Even though the analysis is completed it would be illuminating if we recover analytically the result in two limiting cases. We follow closely [15] by slightly adapting it to the present case.

2.1.1. $J \ll \sqrt{g_s N_c}$ Mesons

Let us analyse the $J \rightarrow 0$ limit. As depicted in fig. 2, the configuration corresponding to very small J is a string that directly stretches in the z direction between both flavour branes, without bending. Obviously, this is qualitatively different of what happens in the single flavour case. In order to have $J \rightarrow 0$, we need $r \rightarrow 0$ (for all the string worldsheet),

^b Even if we plot dots, this by no means is because any quantisation of the angular momenta. Those intent only to be representative points.

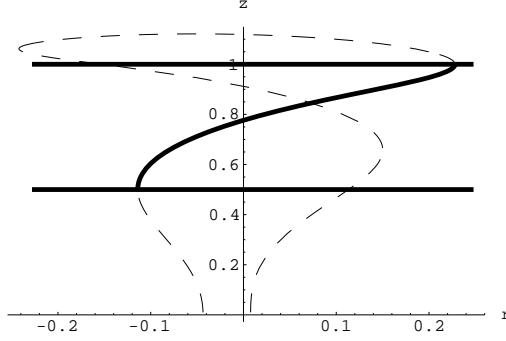


Fig. 2: The profile of the string for $J \ll \sqrt{gsNc}$ for $m_q = 1$, $M_q = 2$ and $\omega = 4$. The dashed lines represent the analytic continuation of the string profile. As suggested in [15] those lines correspond to *gluons shells*. Contrary to the case presented in the above reference in the case of nondegenerate mass these *gluons shells* are not longer symmetric. The horizontal lines represent the probe-branes.

as one can realize after a glance at (2.14). Therefore, we are in the limit corresponding to rotating short strings. Neglecting higher order terms in r , (2.11) becomes

$$r'' - 2\frac{r'}{z} + \omega^2 r = 0, \quad (2.15)$$

with $r(z_{m_q}) = \epsilon$ and where only the leading order in epsilon is taken into account. Supplementing this equation with the boundary conditions $r'(z_{m_q}) = 0$, $r(z_{m_q}) = \epsilon \ll$, we find

$$r(z) = \frac{\epsilon}{z_{m_q} \omega} \left[z\omega \cos((z_{m_q} - z)\omega) + \sin((z_{m_q} - z)\omega) \right]. \quad (2.16)$$

Moreover, by fixing $r'(z_{M_q}) = 0$

$$\omega = \frac{\pi}{z_{m_q} - z_{M_q}}. \quad (2.17)$$

This is a limiting upper value of the angular velocity, contrariwise to the one-mass case, where $\omega \rightarrow \infty$ when $J \rightarrow 0$.

Notice that $m_q r(z_{m_q}) = M_q r(z_{M_q})$. This is the momentum conservation relation for two rotating masses, *i.e.* the string does not carry any energy in this limit acting only as a geometrical constraint.

The energy-spin relation is given in this case by

$$E = M_q - m_q + \frac{2\pi^2 \alpha'}{\mathcal{R}^2} \frac{m_q M_q}{M_q + m_q} J. \quad (2.18)$$

This linear behaviour relating the energy and the angular momentum at high energy has no field theory interpretation.

2.1.2. $J \gg \sqrt{g_s N_c}$ Mesons

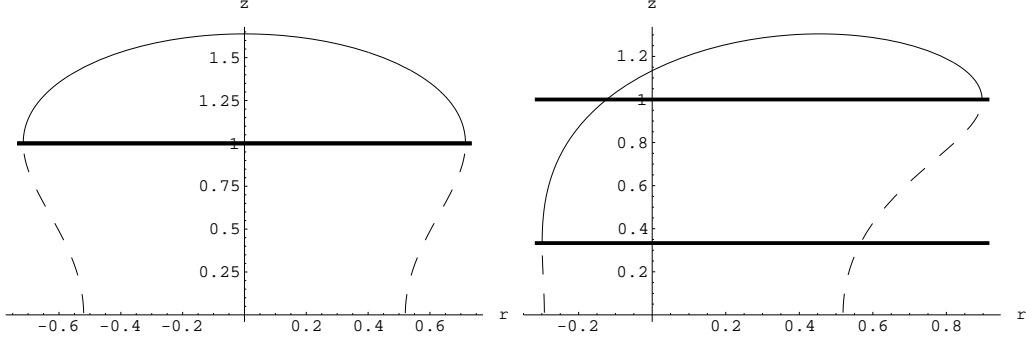


Fig. 3: The $z(r)$ profile for the degenerate, l.h.s., and nonequal mass case, r.h.s. . The dashed lines represent the analytic continuation of the profile following eqs. (2.10), (2.11). The horizontal solid lines represent the two flavour branes. $z = 0$ represents the AdS boundary.

The other possible limit where (2.13) and (2.14) can be tackled analytically is $\omega \rightarrow 0$ which corresponds to rotating long strings that give large J mesons. We shall generalize the analysis of [15] in order to incorporate the effect of having two different quark masses. For small angular velocity, the profile of the string must be similar to that of a static string hanging between both branes. This is given by

$$r_{\text{st}}(z) = r_0 + \int_z^{z_0} dx \frac{x^2}{\sqrt{z_0^4 - x^4}}, \quad (2.19)$$

where $z_0 \rightarrow \infty$ in the limit we are considering and it refers to the extremal point. We have defined r_0 as the r coordinate of the point where the string bends back. It cannot be set to zero as $r = 0$ is by definition the center of rotation of the string and both points do not coincide for nondegenerate masses (see the asymmetric plot in fig. 3). Let us point out that the distance between the string edges is [4,5]

$$r_{m_q} + r_{M_q} = 2\mathcal{C} z_0, \quad (2.20)$$

with

$$\mathcal{C} = \int_1^\infty \frac{dy}{y^2 \sqrt{y^4 - 1}} = \frac{\sqrt{\pi} \Gamma(3/4)}{\Gamma(1/4)}. \quad (2.21)$$

By considering $r(z) = r_{\text{st}}(z) + \delta r(z)$ and keeping the leading order in $\delta r(z)$, ω^2 , (2.11) reads

$$\delta r'' - \frac{2}{z}(1 + 3r_{\text{st}}'^2)\delta r' = -\omega^2 r_{\text{st}} \frac{1 + r_{\text{st}}'^2}{1 - \omega^2 r_{\text{st}}^2}. \quad (2.22)$$

This equation can be straightforwardly integrated

$$\delta r'(z) = \frac{z^2}{(z_0^4 - z^4)^{\frac{3}{2}}} \left[\text{const} + \omega^2 z_0^4 \int_{z_0}^z \frac{\sqrt{z_0^4 - x^4}}{x^2} \frac{r_{\text{st}}(x)}{1 - \omega^2 r_{\text{st}}^2(x)} dx \right], \quad (2.23)$$

and in addition has to be supplemented with the boundary conditions (2.12). They read

$$r'_{\text{st}}(z_{m_q}) + \delta r'(z_{m_q}) = r'_{\text{st}}(z_{M_q}) + \delta r'(z_{M_q}) = 0. \quad (2.24)$$

As we are in the long string regime, one can approximately think on the profile of the string in the following way: It stretches vertically from z_{M_q} to z_0 at constant r_{M_q} , then stretches horizontally from r_{M_q} to r_{m_q} at constant z_0 and finally stretches again vertically from z_0 to z_{m_q} at constant r_{m_q} . A glance at (2.23) reveals that the integral is dominated by the vertical regions *i.e.* $x \ll z_0$. Moreover, the constant can be set to zero as the point with $\delta r' = 0$ is in the horizontal region, at least when the quark masses are of the same order of magnitude (this reasoning fails when $\frac{M_q}{m_q} \rightarrow \infty$, because when there is an infinite mass $r'_{\text{st}}(z_{M_q}) = 0$ so $\delta r'(z_{M_q}) = 0$, *i.e.* the $\delta r' = 0$ point is in the vertical region).

Then, one finds from (2.24)

$$\omega^2 = \frac{z_{m_q}}{r_{m_q} z_0^2} = \frac{z_{M_q}}{r_{M_q} z_0^2}, \quad (2.25)$$

where we have used the relation $z_0 \gg z_{m_q}, z_{M_q}$ and, as can be proved from (2.20), (2.25), $\omega^2 r_{M_q}^2, \omega^2 r_{m_q}^2 \ll 1$. From (2.25) it is immediate that

$$m_q r_{m_q} = M_q r_{M_q}. \quad (2.26)$$

This is the momentum conservation relation for two rotating nonrelativistic masses, and signals that the horizontal part of the string carries a neglectable amount of energy.

Using the relations above, it is easy to compute the angular momentum from (2.14) to leading order

$$J \approx \frac{\mathcal{R}^2 \mathcal{C}}{\pi \alpha' z_0 \omega} + \dots \quad (2.27)$$

The energy (2.13), considering the leading and subleading orders is

$$E \approx \frac{\mathcal{R}^2}{2\pi\alpha'} \left(\frac{1}{z_{m_q}} + \frac{1}{z_{M_q}} - \frac{\mathcal{C}}{z_0} \right) + \dots \quad (2.28)$$

Using (2.20), (2.25) and (2.27) this expression can be recast as

$$E = M_q + m_q - E_{\text{binding}}, \quad E_{\text{binding}} = \frac{2m_q M_q}{(m_q + M_q)} \frac{\kappa^4}{4J^2}, \quad (2.29)$$

where

$$\kappa^4 = \left(\frac{\mathcal{R}^2}{2\pi\alpha'} \right)^2 16 \mathcal{C}^4 = \frac{16}{\pi} g_s N_c \mathcal{C}^4. \quad (2.30)$$

We deal with a system of two nonrelativistic particles bounded in a Coulombic potential, $V(r) \sim -\kappa^2/r$, where only a finite energy cost is needed to separate the two masses. Notice that the binding energy is proportional to the reduced mass of the system. At relatively large separations, $J \gg$, the hadron mass asymptotes to $M_q + m_q$. While for given masses and strong coupling $E_{\text{binding}} \ll (M_q + m_q)$, hence been the string stable. When the limit $M_q \rightarrow \infty$ with m_q held fixed is taken the binding energy must become independent of the coupling [16] and our procedure fails.

2.2. Quark-antiquark energy

The Wilson loop provides an order parameter for pure gluodynamics. Even if in the presence of dynamical quarks this feature is washed out, it still shows a strong sensitivity in the transition region and therefore is widely used to describe crossover in full QCD. A possible gravity analog for infinitely heavy-quarks was presented in [4,5].

The addition of dynamical flavour test sources [6], D7-branes, allows for the inclusion of light-quark masses [17]. It is of interest to investigate the behavior of the $\bar{q}q$ energy as a function of their relative separation in this case. One of the expected new features is the screening in the potential due to light-quarks. To compute the $q\bar{q}$ energy we locate an open string with the two ends on the probe-branes and stretching from them to the origin in the U coordinate. At some point U_0 , before hitting the horizon, it bends back. The relevant part of the metric reduces then to

$$ds^2 = \alpha' \left[\frac{U^2}{\mathcal{R}^2} (-dt^2 + dr^2) + \frac{\mathcal{R}^2}{U^2} dU^2 \right]. \quad (2.31)$$

The string configuration is parametrised as

$$U = U(\sigma), \quad r = \sigma, \quad t = \tau.$$

This leads to the lagrangian density

$$\mathcal{L} = \frac{1}{2\pi\alpha'} \int_{r_{\min}}^{r_{\max}} dr \sqrt{U'^2 + \frac{U^4}{\mathcal{R}^4}}. \quad (2.32)$$

The independence of (2.32) w.r.t. the world-sheet variable σ implies the existence of a conserved quantity

$$\frac{U^4}{\sqrt{U'^2 + \frac{U^4}{\mathcal{R}^4}}} = \mathcal{R}^2 U_0^2. \quad (2.33)$$

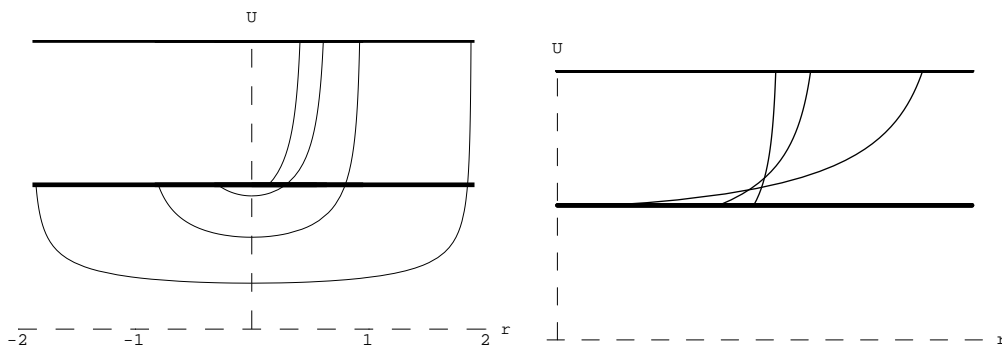


Fig. 4: The profile of the string in the $U - r$ plane for different lengths. The figure on the left corresponds to long strings and the one on the right to short strings. In both cases we take $m_q = 1$, $M_q = 2$

In fig. 4 we have plotted the profile of the string obtained by numerically solving (2.33). For long strings there is a turning point while short strings stretch directly between probe branes. Notice that the long string limit is achieved by approaching $U_0 \rightarrow 0$.

The separation between the two ends of the string can be easily computed from (2.33)

$$L = 2 \frac{\mathcal{R}^2}{U_0} \int_1^{2\pi \frac{m_q}{U_0}} \frac{dy}{y^2 \sqrt{y^4 - 1}} + \frac{\mathcal{R}^2}{U_0} \int_{2\pi \frac{m_q}{U_0}}^{2\pi \frac{M_q}{U_0}} \frac{dy}{y^2 \sqrt{y^4 - 1}}. \quad (2.34)$$

In the latter expression the second term in the r.h.s. is due to the breaking of the mass degeneracy. With the use of (2.34) the energy (2.33) can be casted as

$$E = \frac{U_0}{\pi} \int_1^{2\pi \frac{m_q}{U_0}} dy \frac{y^2}{\sqrt{y^4 - 1}} + \frac{U_0}{2\pi} \int_{2\pi \frac{m_q}{U_0}}^{2\pi \frac{M_q}{U_0}} dy \frac{y^2}{\sqrt{y^4 - 1}}. \quad (2.35)$$

However, notice that (2.34) can only describe configurations for which the string is longer than

$$L_{lim} = \frac{\mathcal{R}^2}{2\pi m_q} \int_1^{\frac{M_q}{m_q}} \frac{dy}{y^2 \sqrt{y^4 - 1}}. \quad (2.36)$$

This value obtained for $U_0 = 2\pi m_q$. For $L < L_{lim}$, the string does never reach values of U smaller than $2\pi m_q$, as can be seen in fig. 4. Therefore, the separation between the string ends and the energy are given simply by

$$L = \frac{\mathcal{R}^2}{U_0} \int_{2\pi \frac{m_q}{U_0}}^{2\pi \frac{M_q}{U_0}} \frac{dy}{y^2 \sqrt{y^4 - 1}}, \quad E = \frac{U_0}{2\pi} \int_{2\pi \frac{m_q}{U_0}}^{2\pi \frac{M_q}{U_0}} dy \frac{y^2}{\sqrt{y^4 - 1}}. \quad (2.37)$$

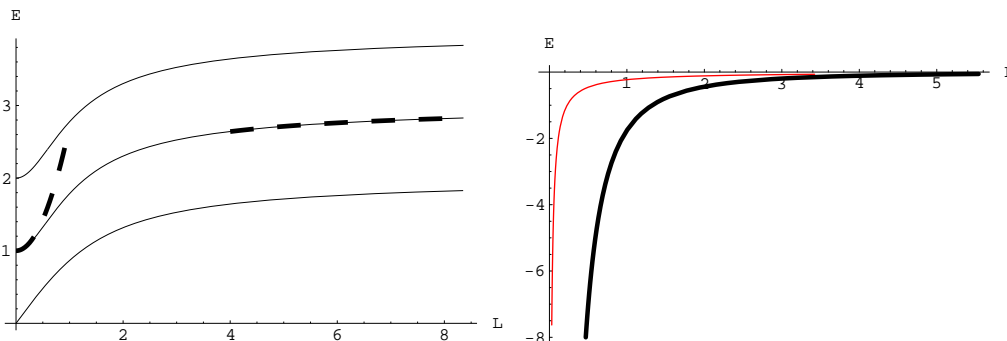


Fig. 5: The energy in terms of the length for $m_q = 1$ and, from bottom to top, $M_q = 1, 2, 3$, l.h.s. For the $M_q = 2$ case we show the asymptotic (2.41) and (2.42). In the right panel we show the case of infinite heavy mass for i) the D3-D7 system (2.38), thin curve and ii) for the D4-D6 system (3.29) thick curve.

In fig. 5, we have plotted the energy as a function of the distance between the string ends. For large L , the effect of incorporating a heavier mass shifts the curves upwards but without modifying its characteristics. But for small L a novel effect w.r.t. the equal mass case appears: instead of a pure linear behaviour there is a slight positive curvature, a *kind of parabola*, that increases with the mass difference. Notice that in this case the slope, as approaching $L \rightarrow 0^+$, decreases indicating a smaller running of the β -function.

2.2.1. Mass Subtraction

Notice that (2.35) is not a renormalised expression, and therefore it will diverge as soon as the upper cutoffs are moved to the boundary at infinity. In that case, we shall deal with an infinitely heavy, degenerate pair of quarks. To render (2.35) finite in this case, we subtract the mass of the static quarks given by a couple of strings, one for each quark, stretching from the boundary to the horizon along the transverse coordinate $U(\sigma) = \sigma$, $X_0 = \tau$ [5]. With this (2.35) reads

$$E_{\text{ren}} = \frac{U_0}{\pi} \left[\int_1^\infty dy \left(\frac{y^2}{\sqrt{y^4 - 1}} - 1 \right) - 1 \right]. \quad (2.38)$$

Different shapes in the string providing the subtraction must correspond to different renormalisation schemes in field theory. We have checked, in the degenerate case, that (2.35) and not the analog of (2.38) for finite masses gives the minimum energy for the string configuration: we locate a pair of quarks, $q\bar{q}$, on the D7-brane with a fixed distance among them, L_0 . The dynamics is purely dictated by the motion of the $q\bar{q}$ system under the potential created by the stack of the D3-branes at the origin. Minimizing (2.35) and (2.38) as a function of m_q , $E(L_0, m_q)$, one can verify that the energy of the system is minimum when (2.35) is used. In increasing m_q to high values the difference between (2.35) and (2.38) is reduced until we reach the limit $m_q \rightarrow \infty$ where the role is interchanged and the energy minimum is given by (2.38).

It is instructive to discuss some approximation to different scales:

2.2.2. Long strings

At low-energy we shall take the following set of assumptions

$$\text{Length} = L \text{ fixed and large}; \quad m_q, M_q \gg 2\pi.$$

Solving iteratively (always at leading order) one can find the turning point for a given string length

$$U_0 = \frac{\mathcal{R}^2}{L} \mathcal{C} \left[2 - \frac{1}{3} \frac{\mathcal{C}^2 \mathcal{R}^6}{(\pi L)^3} \left(\frac{1}{m_q^3} + \frac{1}{M_q^3} \right) \right], \quad (2.39)$$

with \mathcal{C} given in (2.21). For $M_q \rightarrow m_q$ we recover the symmetric case [15]. Corrections due to heavy masses are suppressed.

Within the same approximation the energy gives

$$E = M_q + m_q + \frac{U_0}{\pi} \left[\int_1^\infty dy \left(\frac{y^2}{\sqrt{y^4 - 1}} - 1 \right) - 1 \right] - \frac{U_0}{2\pi} \int_{2\pi \frac{m_q}{U_0}}^\infty dy \left(\frac{y^2}{\sqrt{y^4 - 1}} - 1 \right) - \frac{U_0}{2\pi} \int_{2\pi \frac{M_q}{U_0}}^\infty dy \left(\frac{y^2}{\sqrt{y^4 - 1}} - 1 \right). \quad (2.40)$$

Without performing the limit $M_q, m_q \rightarrow \infty$ there is no need of bare mass subtraction as in [4,5] (see discussion above). Using the leading order in (2.39) we obtain

$$E \approx M_q + m_q - \frac{\kappa^2}{L} \left[1 - \frac{1}{12} \frac{\mathcal{R}^6 \mathcal{C}^2}{(\pi L)^3} \left(\frac{1}{m_q^3} + \frac{1}{M_q^3} \right) \right]. \quad (2.41)$$

Notice that the the binding energy between quarks is attractive and corresponds at leading order to a system of two nonrelativistic particles.

2.2.3. Short strings

We shall consider now the case where the string is short. The limit $L \rightarrow 0$ is clearly achieved by taking $U_0 \rightarrow 0$, (2.37). Then, it is easy to prove that only keeping the first nontrivial contribution of the Taylor expansion of the energy in terms of the string ends separation, one has a quadratic behaviour

$$E = M_q - m_q + \frac{6\pi^2}{\mathcal{R}^4} \left(\frac{1}{m_q^3} - \frac{1}{M_q^3} \right)^{-1} L^2, \quad (2.42)$$

contrariwise to any field theory expectation.

3. QCD₃₊₁: D4-D6 brane model

A more realistic model, in the sense of being four-dimensional and not supersymmetric, can be obtained by placing a stack of N_c D4 branes at the origin and wrapping them on a S^1 cycle. The latter are the source for fermion mass at one loop once antiperiodic b.c. are assumed [18]. As previously we can set an N_f D6-probe branes displaced a distance in some subspace orthogonal to both brane sets.

The field components at leading order in α' are

i) The 10d background metric

$$ds_{10}^2 = \left(\frac{U}{R} \right)^{3/2} \left(-dx_0^2 + dx_1^2 + \dots + dx_3^2 + \frac{4R^3}{9U_h} f(U) d\theta_2^2 \right)$$

$$+ \left(\frac{R}{U}\right)^{3/2} \frac{dU^2}{f(U)} + R^{3/2} U^{1/2} d\Omega_4^2, \quad (3.1)$$

with $f(U) = 1 - \frac{U_h^3}{U^3}$, $R = (\pi N_c g_s)^{1/3} \alpha'^{1/2}$ and U_h denoting the horizon location.

ii) A constant four-form field strength (in string units)

$$F_4 = \frac{3}{8\pi^3 g_s} R^3 \omega_4, \quad (3.2)$$

with ω_4 been the volume form of the transverse S^4 .

iii) Finally, the dilaton field

$$e^\Phi = g_s \left(\frac{U}{R}\right)^{3/4}. \quad (3.3)$$

The relation with the gauge field theory parameters is given by

$$2\pi\lambda = \frac{3R^{3/2}U_h^{1/2}}{\alpha'} = g_{\text{YM}}^2 N_c.$$

To be in the supergravity approximation the following requirements of the fields have to be fulfilled

- i) The smallness of the scalar field (3.3). This restricts the reliability of the background to the infrared region.
- ii) The smallness of the curvature invariant and higher order derivatives.

This two restrictions amounts to take the 't Hooft limit $g_{\text{YM}}^2 N_c \gg 1$.

In addition, in order to describe QCD_{3+1} one has to demand

- iii) that the energy scale is such that its associated transverse coordinate U in the supergravity description corresponds to values where the background is indeed dual to QCD_{3+1} rather than QCD_{4+1} .

The third restriction can be examined from the perspective of the quark-antiquark energy, which will be considered in section (3.3). In fact, it is only in the regime of large distances L between the quark and the antiquark that we reproduce the area law describing the feature of confinement of QCD. At small distances the S^1 opens up and the background no longer describes QCD_{3+1} but QCD_{4+1} . If the position of the $D6$ brane, where the quark-antiquark stay, is far away in the transverse coordinate, we shall deal with a Coulomb phase for the $4 + 1$ field theory. Large distances means that the string of the Wilson loop goes deep into the bulk along the transverse coordinate until it bends in a minimum near the horizon. The bending must occur at some U_0 such that $\frac{U_0 - U_h}{U_h} \ll 1$. This is a third condition that must be met in order to stay in the region

where the background exhibits the area law behaviour for the Wilson loop. Note that this condition will guarantee that $U - U_h \ll M_{kk}$, which is the regime where the theory is effectively four dimensional [19].

Finally, let us point out that the mass of the quark is given by the energy of a string stretching from the horizon to a flavour brane

$$m_q = \frac{1}{2\pi\alpha'} \int_{U_h}^{U_{D6}} \frac{1}{\sqrt{1 - \left(\frac{U_h^3}{U^3}\right)}} dU . \quad (3.4)$$

3.1. Spinning mesons

We turn once more to the analysis of rotating strings. The initial point is (2.3) and the string configuration is identical to (2.6) . The relevant part of the metric is

$$ds^2 = \left(\frac{U}{R}\right)^{3/2} (-dt^2 + dr^2 + r^2 d\theta^2) + \left(\frac{R}{U}\right)^{3/2} \frac{dU^2}{f(U)} . \quad (3.5)$$

That leads to the action [20]

$$S = \frac{1}{2\pi\alpha'} \int d\sigma d\tau \sqrt{U^3 (\kappa^2 - \omega^2 r^2) \left(\frac{U'^2}{U^3 f(U)} + \frac{r'^2}{R^3} \right)} . \quad (3.6)$$

As in the D3-D7 case the variation of the action imposes that the strings end orthogonally to the D6-branes.

In general the e.o.m derived from (3.6) are difficult, if not impossible, to be tackled in an analytic way, but as previously the solutions can simplify by choosing the proper gauge fixing conditions ($\kappa = 1$).

i) $U(\sigma) = \sigma$

$$r'' - \frac{3}{2R^3\sigma} (U_h^3 - \sigma^3) r'^3 + \frac{\omega^2}{1 - \omega^2 r^2} r r'^2 + \frac{3}{2\sigma} \frac{(U_h^3 - 2\sigma^3)}{(U_h^3 - \sigma^3)} r' - \frac{R^3 \omega^2}{(U_h^3 - \sigma^3)(1 - \omega^2 r^2)} r = 0 . \quad (3.7)$$

ii) $r(\sigma) = \sigma$

$$U'' + \frac{R^3 \omega^2 \sigma}{(1 - \omega^2 \sigma^2)(U_h^3 - U^3)} U'^3 - \frac{3}{2U} \left(\frac{U_h^3 - 2U^3}{U_h^3 - U^3} \right) U'^2 - \frac{\omega^2 \sigma}{1 - \omega^2 \sigma^2} U' - \frac{3}{2R^3} \left(\frac{2U_h^3 - U^3}{U_h^3 - U^3} \right) U^2 + \frac{3U_h^6}{2R^3 U (U_h^3 - U^3)} = 0 . \quad (3.8)$$

In addition we impose the b.c. $U_{D6}^{(i)} = \text{fixed}, \partial_\sigma U_{D6}^{(i)}|_{\sigma=\pm\frac{\pi}{2}} \rightarrow \infty, (i = 1, 2)$.

The invariance of (3.6) with respect to t and θ signals the energy and spin conservation

$$E = \frac{1}{2\pi\alpha'} \int d\sigma \left(\frac{U}{R}\right)^{3/2} \sqrt{\frac{r'^2 + \frac{R^3 U'^2}{U^3 - U_h^3}}{1 - (\omega r)^2}}, \quad (3.9)$$

$$J = \frac{\omega}{2\pi\alpha'} \int d\sigma r^2 \left(\frac{U}{R}\right)^{3/2} \sqrt{\frac{r'^2 + \frac{R^3 U'^2}{U^3 - U_h^3}}{1 - (\omega r)^2}}. \quad (3.10)$$

For the rest of this section, we set $2\pi\alpha' = 1$.

3.1.1. Meson spectrum at large J

Once again, the regime of large angular momentum corresponds to long strings rotating with small angular velocity $\omega \rightarrow 0$.

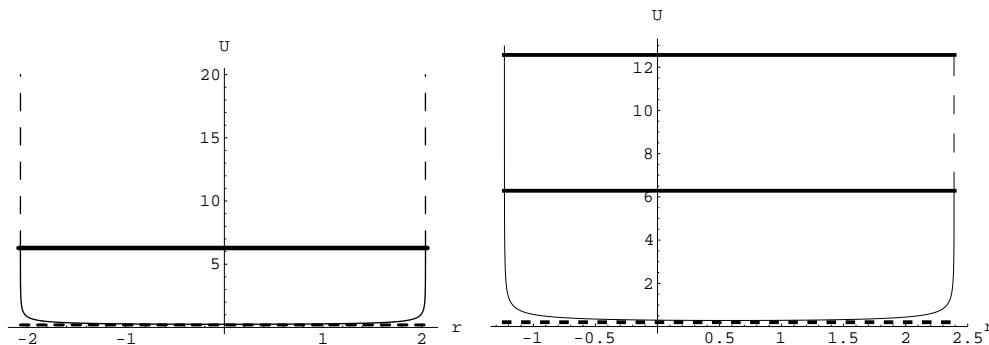


Fig. 6: The profile for long strings, $\omega \rightarrow 0$. Equal mass case and different masses (l.h.s. and r.h.s. respectively). The dotted line denotes the horizon position, the horizontal full lines the flavour brane location and the dashed line the analytic string continuation.

In fig. 6 we show a numerical solution for the string profile. This is approximately given by that of a static long string

$$\partial_U r = (RU_0)^{3/2} \frac{1}{\sqrt{(U^3 - U_0^3)(U^3 - U_h^3)}}, \quad (3.11)$$

which is characterised by *almost* straight strings. Notice that (3.11) diverges in the limit $U_0 \rightarrow U_h$. As previously U_0 denotes the string turning point.

The numerical solutions to (3.7), (3.8) are almost identical to those depicted in fig. 2 and fig. 3. Even possessing these numerical solution is not too much illuminating. As first noticed in [20], an inspection of fig. 6 reveals that for slowly rotating string, $J \gg \sqrt{g_s N_c}$, a good approximation is to consider three parts of the string: two stretching

in the U direction from $U_{D6}^{(1)}$ and $U_{D6}^{(2)}$ to U_h and the third horizontal piece where the string stretches in the field theory directions (r) at $U = U_h$. This allows to split approximately the integrals (3.9), (3.10) in three regions. The two vertical regions, correspond to $r'^2 \ll \frac{R^3 U'^2}{U^3 - U_h^3}$ and the horizontal region ($U \approx U_h$) to $r'^2 \gg \frac{R^3 U'^2}{U^3 - U_h^3}$ *. Therefore, the energy reads

$$\begin{aligned}
E &= \\
\left(\frac{U_h}{R}\right)^{\frac{3}{2}} \int_{-r_{m_q}}^{r_{M_q}} \frac{dr}{\sqrt{1 - \omega^2 r^2}} &+ \frac{1}{\sqrt{1 - \omega^2 r_{m_q}^2}} \int_{U_h}^{U_q} \frac{U^{\frac{3}{2}} dU}{\sqrt{U^3 - U_h^3}} + \frac{1}{\sqrt{1 - \omega^2 r_{M_q}^2}} \int_{U_h}^{U_Q} \frac{U^{\frac{3}{2}} dU}{\sqrt{U^3 - U_h^3}} \\
&= \left(\frac{U_h}{R}\right)^{\frac{3}{2}} \omega^{-1} \left(\arcsin(\omega r_{m_q}) + \arcsin(\omega r_{M_q}) \right) + \frac{m_q}{\sqrt{1 - \omega^2 r_{m_q}^2}} + \frac{M_q}{\sqrt{1 - \omega^2 r_{M_q}^2}}, \quad (3.12)
\end{aligned}$$

whereas the angular momentum can be expressed as

$$\begin{aligned}
J &= \\
\left(\frac{U_h}{R}\right)^{\frac{3}{2}} \int_{-r_{m_q}}^{r_{M_q}} \frac{\omega r^2 dr}{2\sqrt{1 - \omega^2 r^2}} &+ \frac{\omega r_{m_q}^2}{\sqrt{1 - \omega^2 r_{m_q}^2}} \int_{U_h}^{U_q} \frac{U^{\frac{3}{2}} dU}{\sqrt{U^3 - U_h^3}} + \frac{\omega r_{M_q}^2}{\sqrt{1 - \omega^2 r_{M_q}^2}} \int_{U_h}^{U_Q} \frac{U^{\frac{3}{2}} dU}{\sqrt{U^3 - U_h^3}} \\
&= \left(\frac{U_h}{R}\right)^{\frac{3}{2}} \omega^{-2} \left(\arcsin(\omega r_{m_q}) - \omega r_{m_q} \sqrt{1 - \omega^2 r_{m_q}^2} + \arcsin(\omega r_{M_q}) - \omega r_{M_q} \sqrt{1 - \omega^2 r_{M_q}^2} \right) + \\
&\quad + \frac{\omega r_{m_q} m_q}{\sqrt{1 - \omega^2 r_{m_q}^2}} + \frac{\omega r_{M_q} M_q}{\sqrt{1 - \omega^2 r_{M_q}^2}}. \quad (3.13)
\end{aligned}$$

Notice that this is just a straightforward generalization of the results presented in [20]. Hereafter r_{m_q} and r_{M_q} stand for the radius of rotation of the light and heavy quark respectively.

Recall that not all of the parameters in the above expressions are independent. For given values of the masses, once ω is fixed, the values of r_{m_q} , r_{M_q} follow from it as a consequence of the boundary conditions that must be imposed on the string. In order to compute this relation, we will follow the steps of [15] and define

$$r(U) = r_{\text{st}}(U) + \delta r(U), \quad (3.14)$$

where r_{st} stands for the static configuration (3.11). Considering infinitesimal ω^2 , $\delta\rho$ we can expand (3.7) and get a first order differential equation in $\delta r'(U)$

$$(U^3 - U_0^3)(U^3 - U_h^3)\delta r'' + \frac{3\delta r'}{2U}(U^3(U_0^3 - U_h^3) + 2U^6 - U_0^3 U_h^3) + \frac{\omega^2 r_{\text{st}}(U)}{1 - \omega^2 r_{\text{st}}^2(U)} R^3 U^3 = 0, \quad (3.15)$$

* In order to see this, consider $\sigma = U$, so both terms go to infinity but the first one dominates as the string profile at small ω must be similar to the static one, so (3.11) holds approximately.

which can be immediately integrated

$$\delta r'(U) = \frac{U^3}{(U^3 - U_0^3)^{\frac{3}{2}}(U^3 - U_h^3)^{\frac{1}{2}}} \left(-R^3 \omega^2 \int_{U_{\text{ref}}}^U \frac{\sqrt{x^3 - U_0^3}}{\sqrt{x^3 - U_h^3}} \frac{r_{\text{st}}(x)}{1 - \omega^2 r_{\text{st}}(x)^2} dx \right). \quad (3.16)$$

The integration constant has been encoded in U_{ref} , that we define as the value of U at which $\delta r'(U) = 0$. The boundary conditions are that both ends of the string reach both flavour branes orthogonally (2.12)

$$r'(U_{D6}^{(i)}) = r'_{\text{st}}(U_{D6}^{(i)}) + \delta r'(U_{D6}^{(i)}) = 0. \quad (3.17)$$

As we are in the long string regime, $U_0 \approx U_h$ and the integral in (3.16) is dominated by the vertical part of the string. Moreover, unless $\frac{M_q}{m_q} \rightarrow \infty$, one can safely $U_{\text{ref}} \approx U_0$ as the point where the derivative does not get modified must be in the horizontal region of the string. In the degenerate case $m_q = M_q$, one has just $U_{\text{ref}} = U_0$ because of the symmetry. The relevant integral is, then $\int_{U_0}^{U_{D6}} \frac{r_{\text{st}}(x)}{1 - \omega^2 r_{\text{st}}(x)^2} dx \approx \frac{r}{1 - \omega^2 r^2} (U_{D6} - U_h)$. From (3.17), one gets two conditions[†]

$$1 - \omega^2 r_{m_q}^2 = T_s^{-1} \omega^2 r_{m_q} \tilde{m}_q, \quad 1 - \omega^2 r_{M_q}^2 = T_s^{-1} \omega^2 r_{M_q} \tilde{M}_q, \quad (3.18)$$

where T_s is the tension of a string stretched at $U = U_h$

$$T_s = \left(\frac{U_h}{R} \right)^{\frac{3}{2}} \quad (3.19)$$

and we have defined for each quark

$$\tilde{m} = \frac{(U_{D6} - U_h) U_{D6}^3}{U_{D6}^3 - U_h^3}. \quad (3.20)$$

Notice that for $U_{D6} \gg U_h$, one has $\tilde{m} \approx m$ (3.4), *i.e.* the mass of the quark, recovering the results of [20], which are the holographic realization of the hadron model of a relativistic string rotating in flat space [21,22]. Identifying \tilde{m}, \tilde{M} with the mass of the quarks, (3.18) ensures the conservation of the center of mass motion for a rotating string with massive endpoints attached [21]

$$\frac{m_q r_{m_q} \omega}{\sqrt{1 - r_{m_q}^2 \omega^2}} - \frac{T_s}{\omega} \sqrt{1 - r_{m_q}^2 \omega^2} = \frac{M_q r_{M_q} \omega}{\sqrt{1 - r_{M_q}^2 \omega^2}} - \frac{T_s}{\omega} \sqrt{1 - r_{M_q}^2 \omega^2}. \quad (3.21)$$

[†] Notice, however, that the procedure to obtain the constraints (3.18) differs from that in [20]. In [20], the string was cut into three pieces and (3.18) is the condition for a proper gluing of the three pieces. Here, the string was treated as a whole and (3.18) comes from the boundary condition of the ends of the string hitting the branes orthogonally.

This is certainly signaling that gluons inside the flux tube play a *dynamical* role and not only act as a mere geometric constraint, contributing to the total energy of the system. If not, momentum conservation would be just (consider $r_{m_q}^2 \omega^2 \ll 1$)

$$m_q r_{m_q} = M_q r_{M_q}, \quad (3.22)$$

as in the supersymmetric case. In this nonrelativistic limit, the momentum conservation (3.21) reads

$$m_q r_{m_q} + \frac{T_s}{2} r_{m_q}^2 = M_q r_{M_q} + \frac{T_s}{2} r_{M_q}^2. \quad (3.23)$$

We expect a smooth transition between both behaviours, (3.22), and (3.23).

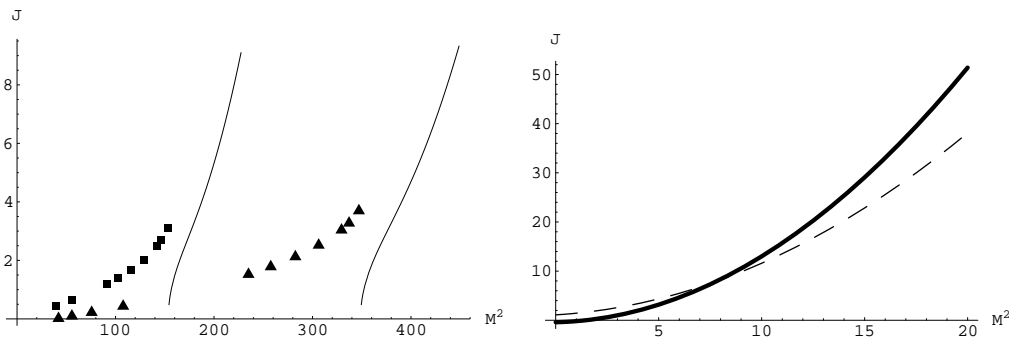


Fig. 7: Chew-Frautschi plot obtained numerically for $U_h = .2$, $U_{D6(1)} = 2\pi$ and $U_{D6(2)} = 2\pi$ (squares), $U_{D6(2)} = 4\pi$ (triangles). The solid lines obtained using (3.12), (3.13), (3.18) are the extrapolation of these curves to the large- J region. For comparison in the r.h.s. we have plotted the experimental nucleon (full curve) [23] and Pomeron (dashed) [24] Regge trajectories.

In fig. 7, we have depicted the Chew-Frautschi corresponding to this model. The curves giving the large- J limit are represented along with some points obtained numerically from (3.7), (3.8), (3.9), (3.10) in the region of intermediate J . Unfortunately, we have not been able to perform a trustable numerical analysis of the very large- J region, because when the string has a nearly vertical-horizontal-vertical profile, numerical instabilities appear. Despite the long extrapolation, the numerical results are robust and trustable in the intermediate range of J we considered. For comparison in the r.h.s., we have presented some experimental data. Notice that the qualitative similitude with the l.h.s. in the full region is remarkable.

Given the above naive picture it is tempting to think in a very special limit of QCD, heavy quark effective theory, consisting of heavy hadrons composed by one heavy quark and one light one [25]. The heavy quark momenta is given by $P_Q^\mu = m_Q v_Q^\mu + k^\mu$, been

k^μ a residual momenta of order Λ_{QCD} , while the hadron total momenta is $P_H^\mu = m_H v^\mu$. In the heavy quark limit, the velocity superselection rule leads that the residual momenta is negligible and all the hadron momenta is carried by the heavy quark, $P_H \approx P_Q$ [26]. This setup is certainly susceptible to be obtained by the above model using (3.23) via the identification

$$k^\mu \rightarrow m_q r_{m_q} + \frac{T_s}{2} r_{m_q}^2 \approx \mathcal{O}(\Lambda_{QCD}). \quad (3.24)$$

Notice that (3.24) is suggesting that for a given mass the average position of the light-quark with respect to the heavy one is not arbitrary.

3.1.2. Intermediate J strings

In the region of intermediate J , the holographic model differs from the string rotating in flat space [20,21,22] because the string profile cannot be approximated any more by vertical and horizontal regions. It may be regarded as a string of nonconstant tension rotating in flat space. Similar models were considered in [27] in the search of more realistic models. Here, the deviations from the constant tension are given uniquely by the dynamics of the rotating string of the ten-dimensional theory. In fig. 7, the points obtained numerically show the deviation of the formulae computed in the large angular momentum approximation when J goes to intermediate values.

It is tempting to consider these deviations as the holographic realization of the corresponding ones in QCD. However, one should keep in mind that out of the large- J limit, quantum corrections to the semi-classical model must also be taken into account. These kind of corrections were computed in [28] for a static configuration. Our setup is much more involved so it seems hopeless to perform the analogous computation.

3.1.3. Small J strings

For completeness, let us consider the $J \rightarrow 0$ limit, *i.e.* rotating short strings. However, when the string is short, it probes the KK direction, so one cannot think of this setup as the holographic small- J dual of QCD_{3+1} . By taking $r \rightarrow 0$ in (3.7) one finds

$$r'' - \frac{3}{2U} \frac{U_h^3 - 2U^3}{U_h^3 - U^3} r' - \frac{R^3 \omega^2}{U_h^3 - U^3} r = 0. \quad (3.25)$$

We have not been able to find an explicit solution for this equation. However, a numerical computation shows that the qualitative features are similar to those of section 2.1.1. for the supersymmetric case (see fig. 2).

3.2. Quark-antiquark energy

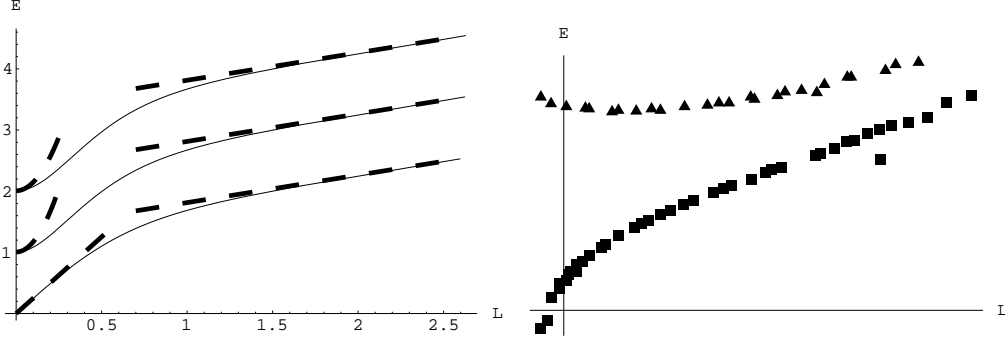


Fig. 8: The quark-antiquark potential as a function of the distance for flavoured branes with, from bottom to top, $m_q = 1$ and $M_q = 1, 2, 3$. We also show the asymptotic limits (3.30), (3.32) and (3.34). The r.h.s. shows for comparison the unquenched lattice results [29]. The squares denote the ground state static potential while triangles stand for the first excited state.

In this section we change tack, retreating from the semi-classical limit of spinning strings to make qualitative statements about the behavior of the static quark potential.

The D6 brane configuration has its world-volume along x_0, x_1, x_2, x_3 and along two coordinates of the S^4 . The setup is realized by the string configuration

$$U = U(\sigma), \quad X_0 = \tau, \quad X_3 = \sigma, \quad (3.26)$$

where we have stuck to the static-gauge. The expressions for the energy and the quark-antiquark separation are basically the same as those obtained in [30] but with an ultraviolet cutoff, equal to the positions of the quarks on the D6-branes

$$L = 2 \frac{R^{3/2}}{U_0^{1/2}} \int_1^{\frac{U_{D6}^{(1)}}{U_0}} dy \frac{1}{\sqrt{(y^3 - 1)(y^3 - \eta^3)}} + \frac{R^{3/2}}{U_0^{1/2}} \int_{\frac{U_{D6}^{(1)}}{U_0}}^{\frac{U_{D6}^{(2)}}{U_0}} dy \frac{1}{\sqrt{(y^3 - 1)(y^3 - \eta^3)}}, \quad (3.27)$$

$$E = \frac{U_0}{\pi} \int_1^{\frac{U_{D6}^{(1)}}{U_0}} dy \frac{y^3}{\sqrt{(y^3 - 1)(y^3 - \eta^3)}} + \frac{U_0}{2\pi} \int_{\frac{U_{D6}^{(1)}}{U_0}}^{\frac{U_{D6}^{(2)}}{U_0}} dy \frac{y^3}{\sqrt{(y^3 - 1)(y^3 - \eta^3)}}, \quad \eta = \frac{U_h}{U_0}. \quad (3.28)$$

In fig. 8 we display the relation energy versus distance in the $q\bar{q}$ system for a given pair $(U_{D6}^{(1)}, U_{D6}^{(2)})$. The gross features for the ground state, convexity, match those of QCD [31] but with a relevant salient point: the existence of a linear behavior at large distances (see discussion below). As in the D3-D7 case the mass splitting only shifts upwards the curve E vs. L in the large L region without introducing any other change. At high-energy the nondegenerate case shows once more a parabolic behaviour. In fact the profile of the l.h.s. plot is identical to the one in the supersymmetric case.

3.2.1. Mass Subtraction

As in the supersymmetric case the energy (3.28) is not a renormalised expression once the integral upper cutoff go to the boundary, and needs subtraction. With the same procedure as previously (3.28) reads

$$E_{\text{ren}} = \frac{U_0}{\pi} \int_1^\infty dy \frac{y^3}{\sqrt{(y^3-1)(y^3-\eta^3)}} - \frac{U_0}{\pi} \int_\eta^\infty dy \sqrt{\frac{y^3}{y^3-\eta^3}}. \quad (3.29)$$

Which, incidentally, does not match with the results of [30].

As it is shown in [17], and unlike in the conformal case, now the D6-brane is not located at a fixed point in the transverse U variable, but rather bends outwards in the region where it is closest to the $D4$ stack of branes. We have checked that the $q\bar{q}$ system minimizes its total energy when located at the place in the D6-brane that minimizes its distance with respect to the $D4$. This result coincides with the conclusions in [17]. In addition, as previously, in order to obtain a light, finite $q\bar{q}$ system we have to make use of (3.28) instead of (3.29).

3.2.2. Long and short strings

We turn to discuss the behaviour of long and short strings. Notice, however, that although the relative distance between the location of the $q\bar{q}$ pair on the D6-brane and the horizon can be small, this by no means leads to the conclusion that the distance between q and \bar{q} must be short as one can indeed verify from (3.27) by approaching the horizon at fixed $U_{D6}^{(i)}$, i.e. $y \rightarrow 1$. In fact for $\eta, y \rightarrow 1$ (3.27) develops a single pole that can not be cured, and hence the string approaches an infinite length.

Long strings

A feature matching the expected QCD behavior is found at low-energy. There the $q\bar{q}$ system has been hadronised and from the macroscopic point of view we deal with hadrons. The slope of these strings is constant. This is consistent with the Regge behaviour shown for rotating long strings in section 3.1.1. In order to obtain long strings at a given finite distance for $U_{D6}^{(i)} \gg (i = 1, 2)$ the string turning point should approach the horizon. In that case $\eta = 1 + \epsilon$ and the relation between the energy and the length along the brane takes the form

$$E = \frac{1}{2\pi} \left(\frac{U_h}{R} \right)^{3/2} L + \frac{1}{2\pi} \left(U_{D6}^{(1)} + U_{D6}^{(2)} - 2U_h \right). \quad (3.30)$$

Notice that the inclusion of heavy masses shifts the intercept but does not modify the slope, thus we still deal a Regge behaviour as in the case of static quarks [30]. The string tension is the same as the one obtained in [30], and matches the expression obtained from

the energy formula for rotating strings [19]. The reason is that at large distances the main contribution to the integrals (3.27), (3.28) comes from the vicinity of the horizon, so the result is insensitive to the presence of the cutoff at $U_{D6}^{(i)}$.

Short strings

As in the supersymmetric case, when the QCD string is very short, its holographic dual is given by a string directly stretching between both flavour branes, without bending (see fig. 4). Then, the expressions for the distance between the ends of the string and its energy are just

$$L = \frac{R^{3/2}}{U_0^{1/2}} \int_{\frac{U_{D6}^{(1)}}{U_0}}^{\frac{U_{D6}^{(2)}}{U_0}} dy \frac{1}{\sqrt{(y^3 - 1)(y^3 - \eta^3)}}, \quad E = \frac{U_0}{2\pi} \int_{\frac{U_{D6}^{(1)}}{U_0}}^{\frac{U_{D6}^{(2)}}{U_0}} dy \frac{y^3}{\sqrt{(y^3 - 1)(y^3 - \eta^3)}}. \quad (3.31)$$

Clearly, the $L \rightarrow 0$ corresponds to taking the integration limit $U_0 \rightarrow 0$ (notice that this makes sense since in this case U_0 does not have the physical meaning of the string turning point). Then, as in the supersymmetric case, one can check that, at leading order, the energy has a parabolic dependence on the distance

$$E = C_1 + C_2 L^2 + \dots, \quad (3.32)$$

where the constants are given by

$$C_1 = \frac{1}{2\pi} \int_{U_{D6}^{(1)}}^{U_{D6}^{(2)}} dx \frac{x^{\frac{3}{2}}}{\sqrt{x^3 - U_h^3}} = M_q - m_q, \quad C_2 = \frac{1}{2\pi R^3} \left(\int_{U_{D6}^{(1)}}^{U_{D6}^{(2)}} dx \frac{1}{x^{\frac{3}{2}} \sqrt{x^3 - U_h^3}} \right)^{-1}. \quad (3.33)$$

For the sake of completeness, let us mention that, in the degenerate case, this reasoning is clearly not valid and the string must stretch with bending. Then, the leading order expansion leads to a constant slope behaviour for the energy

$$E = \frac{1}{2\pi} \left(\frac{U_h}{R} \right)^{3/2} L + \dots. \quad (3.34)$$

This shape has been quite long discussed in QCD, see for instance [32]. With the range of energy explored in the actual lattice data this effect can be interpreted as a renormalon artefact and has no further physical consequences. In the present case we can understand it in an energy basis: in the coordinates (3.1) $E \sim U$. As we increase the U coordinate also the energy is increased. At certain energy, $E \sim M_{KK} \sim \frac{2}{3} \frac{R^{3/2}}{U_0^{1/2}}$ there is an opening of the dimension on the S^1 , thus we deal with QCD_{4+1} instead of QCD_{3+1} .

To substantiate this claim in an analytic way, we have performed the limit $U_{D6}^{(i)} \rightarrow \infty$, and renormalised the energy with the subtraction (3.29). We can observe that for small distances between the quarks, the energy behaves as

$$E \approx -\eta U_0^{1/2} \frac{1}{L^2} + \text{ct.},$$

thus showing a Coulomb phase for QCD_{4+1} .

3.3. Quark-antiquark potential screening

It is instructive to gain some insight on the effects of including the dynamical quarks, mimicked for the D6-brane. In fig. 5, r.h.s., we have plotted (thick curve) the quark-antiquark energy obtained by taking $U_{D6} \rightarrow \infty$ and subtracting the bare mass (3.29). As one can see, already keeping the effective field theory in (3+1)d, the effect of introducing dynamical quarks is quite noticeable and with similar pattern to the supersymmetric case. This change of behaviour can be understood as a screening effect: while in a pure glue dynamic system composed of two infinite external heavy-quarks the interaction can be only mediated via gluons, in a system with fundamental matter the gluon propagator itself is *dressed* with quarks. This fact weakens the interaction between the valence-quarks and the potential wall gets broadest. To manifest this effect we have fitted to fig. 8, inside the (3+1)d region, two phenomenological models for the case $m_q = M_q = 1$. The first model is given by the screened potential [33]

$$V(r) = \left(-\frac{\alpha}{r} + \sigma r\right) \frac{1 - e^{-\mu r}}{\mu r}, \quad (3.35)$$

and the second by the well-known Cornell potential

$$V(r) = V_0 + br - \frac{a}{r}. \quad (3.36)$$

In this case the model realised with D6-branes behaves most as a screened system at short distances. Although the relative difference between potentials is so small that no conclusive statement on the behaviour of the system can be obtained. Similar conclusions are achieved by lattice studies [34,35].

As a concluding remark on this section we mention that for both, the singlet and the first excited state, see the UV region in fig. 8, the beta function for the D4-D6 system has an UV fixed point. This in the singlet case is in clear contrast with our actual knowledge on perturbative QCD.

3.4. 't Hooft line: monopole-monopole interaction

A complementary way of looking at confinement is via the magnetic dual of the quark, the monopole. The configuration realizing a magnetic monopole from (3.1) is that of a D2-brane ending on the initial D4-brane. The monopole is obtained by wrapping the D2-brane on the compactified S^1 [36,37]. With our conventions, the mass of a free monopole is

$$m_m = K (U_{(D6)} - U_h), \quad (3.37)$$

where we have defined the constant $K \equiv 4\pi T_{D2} R^{3/2} U_h^{-1/2} g_s^{-1}$. The potential between the monopoles is obtained by placing two monopoles at distance L in the x_1 -axis. Consider a

D2-brane parametrised in term of $(t, U(x_1), \theta_2)$. The induced metric on the brane is then [38]

$$g_{tt} = - \left(\frac{U}{R} \right)^{3/2}, \quad g_{UU} = \left(\frac{R}{U} \right)^{3/2} f(U)^{-1} \left(1 + \left(\frac{U}{R} \right)^3 f(U) x_1'(U)^2 \right),$$

$$g_{\theta_2 \theta_2} = \left(\frac{U}{R} \right)^{3/2} \frac{4 R^3}{9 U_h} f(U).$$

Inserting it in the D2 action

$$E_{m-m} = T_{D2} \int dx_1 d\theta_2 e^{-\phi} \sqrt{g_{tt} g_{UU} g_{\theta_2 \theta_2}}, \quad (3.38)$$

we can extract the distance between the ends of the flux-tube and the energy stored in it (for simplicity, we consider monopoles with degenerate mass)

$$L = 2 \frac{R^{3/2}}{U_h^{1/2}} \int_1^{\frac{U_{D6}}{U_0}} \frac{\sqrt{\eta(1-\eta^3)}}{\sqrt{(y^3-1)(y^3-\eta^3)}}, \quad (3.39)$$

$$E = K U_0 \int_1^{\frac{U_{D6}}{U_0}} dy \sqrt{\frac{y^3 - \eta^3}{y^3 - 1}}, \quad (3.40)$$

where η is defined as in (3.28).

For small distance there is a configuration of the flux tube between the monopoles for which the energy (3.40) is less than that of two free monopoles (3.37). As we increase the distance between the monopoles the energy stored in the tube grows up to certain L_{crit} where it reaches $2m_m$ signaling the breaking of the flux tube. From these the most stable configuration corresponds to two flux tubes stretching from each of the monopoles in the D6-brane up to the horizon. This leads to a constant energy density in accordance with field theory expectations [39].

Notice that for probe branes near the horizon, light-quark masses, the breaking takes place at lower values of L_{crit} , while for probe branes supporting heavy quarks the breaking occurs at higher ones.

4. Summary

By considering open rotating strings attached to probe branes we have evaluated semi-classically some properties of a system mimicking excited mesons formed by different constituents masses. We focused on two basic aspects: *i*) the Chew-Frautschi plot and *ii*) the $q\bar{q}$ system energy. The first quantity is obtained by introducing open rotating strings with ends attached to an embedded probe brane an extending into a transverse

coordinate. While the second is a static quantity. In the actual range of energies the QCD static potential has the form

$$V_{q\bar{q}}(r) = -\frac{e}{r} + cr.$$

Adding light flavours we move away of this limit and new effects, as the spin, play an essential role. These potentials are reliable to study heavy quark interaction, but when light quarks are involved, relativistic effects are important and even the concept of inter-quark *potential* remains questioned.

Bearing this lack in mind we construct a system composed by two different, tuneable masses by adding two probe branes and separating them in a plane orthogonal to the initial brane stack world-volume.

The first case of backgrounds we treated is a supersymmetric setup, the D3-D7 brane system, generalising the extremal case [15]. At low-energy neither the $J - E$ relation nor the $E - L$ show a qualitative difference with respect to the degenerate case but at moderate-high energy differences are substantial. Notice that at qualitative level, and without any apparent reason, the $J - E$ and $E - L$ plots show the same shape, see fig. 1, fig. 5.

The second studied background is non-supersymmetric and is obtained considering a thermal cycle in 10d. The gross features of the Chew-Frautschi plot for hadronised systems resembles that of heavy-quarkonia in QCD. The $E - L$ relation presents a Regge type behaviour for large separations, matching the field theory expectations. At high-energy there is however also a Regge behaviour in the case of degenerate masses. This result can be interpreted, *granus salis*, as the possible presence of a screening effect as one can see by fitting the $q\bar{q}$ energy to two different potentials. There is however a rather surprising quantitative agreement with lattice findings if the singlet and 1st excited states are considered. The basic tenets of the model can be tested by lattice Monte-Carlo simulations of higher excited states. The last remark we have made on confinement concerns the picture of a monopole-monopole condensation, which fulfills the field theory expectations.

We stress that the all the mentioned features are independent of having implemented supersymmetry in the theory. In this respect we believe that the aforementioned characteristics of the Chew-Frautschi plot or in the quark-antiquark potential in the D4-D8 [40] model must led to the same qualitative results as those in the D4-D6. Nevertheless it would be interesting to see if the existence, at large-energy, of a Regge behaviour persists in this model.

Acknowledgements

We would like to thank Ll. Ametller, A. Cotrone, C. Núñez, J. M. Pons and A. Rimallo for comments. The work of A. P. was partially supported by INTAS grant, 03-51-6346, CNRS PICS # 2530, RTN contracts MRTN-CT-2004-005104 and MRTN-CT-2004-

503369 and by a European Union Excellence Grant, MEXT-CT-2003-509661. The work of P. T. is supported in part by the European Community's Human Potential Programme under contract MRTN-CT-2004-005104 'Constituents, fundamental forces and symmetries of the universe'.

References

- [1] A. A. Abrikosov, “On The Magnetic Properties Of Superconductors Of The Second Group,” *Sov. Phys. JETP* **5**, 1174 (1957) [*Zh. Eksp. Teor. Fiz.* **32**, 1442 (1957)].
- [2] H. B. Nielsen and P. Olesen, “Vortex-Line Models For Dual Strings,” *Nucl. Phys. B* **61**, 45 (1973).
- [3] A. Zhang, “Regge trajectories analysis to $D^*/sJ(2317)^{+-}$, $D/sJ(2460)^{+-}$ and $D/sj(2632)^+$ mesons,” arXiv:hep-ph/0408124.
- [4] S. J. Rey and J. T. Yee, “Macroscopic strings as heavy quarks in large N gauge theory and anti-de Sitter supergravity,” *Eur. Phys. J. C* **22**, 379 (2001) [arXiv:hep-th/9803001].
- [5] J. M. Maldacena, “Wilson loops in large N field theories,” *Phys. Rev. Lett.* **80**, 4859 (1998) [arXiv:hep-th/9803002].
- [6] A. Karch and E. Katz, “Adding flavor to AdS/CFT,” *JHEP* **0206**, 043 (2002) [arXiv:hep-th/0205236].
- [7] C. Bachas and M. Petropoulos, “Anti-de-Sitter D-branes,” *JHEP* **0102**, 025 (2001) [arXiv:hep-th/0012234].
- [8] A. Karch and L. Randall, “Open and closed string interpretation of SUSY CFT’s on branes with boundaries,” *JHEP* **0106**, 063 (2001) [arXiv:hep-th/0105132].
- [9] L. Ya. Glozman, “Chiral and $U(1)_A$ restorations high in the hadron spectrum, semiclassical approximation and large N_c ,” arXiv:hep-ph/0411281.
- [10] C. Nunez, A. Paredes and A. V. Ramallo, “Flavoring the gravity dual of $N = 1$ Yang-Mills with probes,” *JHEP* **0312**, 024 (2003) [arXiv:hep-th/0311201].
- [11] P. Ouyang, “Holomorphic D7-branes and flavored $N = 1$ gauge theories,” *Nucl. Phys. B* **699**, 207 (2004) [arXiv:hep-th/0311084].
- [12] D. Arean, D. Crooks and A. V. Ramallo, “Supersymmetric probes on the conifold,” *JHEP* **0411**, 035 (2004) [arXiv:hep-th/0408210].
- [13] S. Kuperstein, “Meson spectroscopy from holomorphic probes on the warped deformed conifold,” arXiv:hep-th/0411097.
- [14] J. Babington, J. Erdmenger, N. J. Evans, Z. Guralnik and I. Kirsch, “Chiral symmetry breaking and pions in non-supersymmetric gauge / gravity duals,” *Phys. Rev. D* **69**, 066007 (2004) [arXiv:hep-th/0306018].
- [15] M. Kruczenski, D. Mateos, R. C. Myers and D. J. Winters, “Meson spectroscopy in AdS/CFT with flavour,” *JHEP* **0307**, 049 (2003) [arXiv:hep-th/0304032].
- [16] A. Karch, E. Katz and N. Weiner, “Hadron masses and screening from AdS Wilson loops,” *Phys. Rev. Lett.* **90**, 091601 (2003) [arXiv:hep-th/0211107].
- [17] M. Kruczenski, D. Mateos, R. C. Myers and D. J. Winters, “Towards a holographic dual of large- $N(c)$ QCD,” arXiv:hep-th/0311270.

- [18] E. Witten, “Anti-de Sitter space, thermal phase transition, and confinement in gauge theories,” *Adv. Theor. Math. Phys.* **2**, 505 (1998) [arXiv:hep-th/9803131].
- [19] J. M. Pons, J. G. Russo and P. Talavera, “Semiclassical string spectrum in a string model dual to large N QCD,” *Nucl. Phys. B* **700**, 71 (2004) [arXiv:hep-th/0406266].
- [20] M. Kruczenski, L. A. P. Zayas, J. Sonnenschein and D. Vaman, “Regge trajectories for mesons in the holographic dual of large-N(c) QCD,” arXiv:hep-th/0410035.
- [21] M. Ida, “Relativistic motion of massive quarks joined by a massless string”, *Progr. Theor. Phys.* **59**, 1661 (1978).
- [22] A. Chodos and C. B. Thorn, “Making The Massless String Massive,” *Nucl. Phys. B* **72**, 509 (1974).
- [23] V. A. Lyubimov, “Backward Scattering Of Pions On Nucleons,” *Sov. Phys. Usp.* **20**, 691 (1977) [*Usp. Fiz. Nauk* **123**, 3 (1977)].
- [24] A. Brandt *et al.* [UA8 Collaboration], “Measurements of single diffraction at $s^{*(1/2)} = 630\text{-GeV}$: Evidence for a non-linear $\alpha(t)$ of the pomeron,” *Nucl. Phys. B* **514**, 3 (1998) [arXiv:hep-ex/9710004].
- [25] N. Isgur and M. B. Wise, “Weak Decays Of Heavy Mesons In The Static Quark Approximation,” *Phys. Lett. B* **232**, 113 (1989).
- [26] H. Georgi, “An Effective Field Theory For Heavy Quarks At Low-Energies,” *Phys. Lett. B* **240**, 447 (1990).
- [27] L. Burakovsky, “String model for analytic nonlinear Regge trajectories”, hep-ph/9904322.
- [28] F. Bigazzi, A. Cotrone, L. Martucci and L. Pando Zayas, “Wilson loop, Regge trajectory and hadron masses in a Yang- Mills theory from semiclassical strings”, hep-th/0409205.
- [29] G. S. Bali *et al.* [TXL Collaboration], “Static potentials and glueball masses from QCD simulations with Wilson sea quarks,” *Phys. Rev. D* **62**, 054503 (2000) [arXiv:hep-lat/0003012].
- [30] A. Brandhuber, N. Itzhaki, J. Sonnenschein and S. Yankielowicz, “Wilson loops, confinement, and phase transitions in large N gauge theories from supergravity,” *JHEP* **9806**, 001 (1998) [arXiv:hep-th/9803263].
- [31] C. Bachas, “Convexity Of The Quarkonium Potential,” *Phys. Rev. D* **33**, 2723 (1986).
- [32] M. N. Chernodub, F. V. Gubarev, M. I. Polikarpov and V. I. Zakharov, “Confinement and short distance physics,” *Phys. Lett. B* **475**, 303 (2000) [arXiv:hep-ph/0003006].
- [33] K. D. Born, E. Laermann, N. Pirsch, T. F. Walsh and P. M. Zerwas, “Hadron Properties In Lattice QCD With Dynamical Fermions,” *Phys. Rev. D* **40**, 1653 (1989).
- [34] U. M. Heller, K. M. Bitar, R. G. Edwards and A. D. Kennedy, “The Heavy quark potential in QCD with two flavors of dynamical quarks,” *Phys. Lett. B* **335**, 71 (1994) [arXiv:hep-lat/9401025].

- [35] K. D. Born, E. Laermann, R. Sommer, P. M. Zerwas and T. F. Walsh, “The Interquark potential: A QCD lattice analysis,” *Phys. Lett. B* **329**, 325 (1994).
- [36] A. Hanany and E. Witten, “Type IIB superstrings, BPS monopoles, and three-dimensional gauge dynamics,” *Nucl. Phys. B* **492**, 152 (1997) [arXiv:hep-th/9611230].
- [37] D. E. Diaconescu, “D-branes, monopoles and Nahm equations,” *Nucl. Phys. B* **503**, 220 (1997) [arXiv:hep-th/9608163].
- [38] D. J. Gross and H. Ooguri, “Aspects of large N gauge theory dynamics as seen by string theory,” *Phys. Rev. D* **58**, 106002 (1998) [arXiv:hep-th/9805129].
- [39] N. S. Manton, “The Force Between ’T Hooft-Polyakov Monopoles,” *Nucl. Phys. B* **126**, 525 (1977).
- [40] T. Sakai and S. Sugimoto, “Low energy hadron physics in holographic QCD,” arXiv:hep-th/0412141.